

# A Kinetic-MHD Model for Studying Low Frequency Multiscale Phenomena

C. Z. Cheng and Jay R. Johnson

Princeton Plasma Physics Laboratory

Princeton University, Princeton, New Jersey 08543

## Abstract

A nonlinear kinetic-MHD model for studying low frequency (with frequency less than ion cyclotron frequency) multiscale phenomena has been developed by taking advantage of the simplicity of the single fluid MHD model and by properly taking into account core ion finite Larmor radius (FLR) effects and major kinetic effects of energetic particles. The kinetic-MHD model treats the low energy core plasma by a generalized MHD description and energetic particles by kinetic approach such as the gyrokinetic equation or Vlasov equation, and the coupling between the dynamics of these two components of plasmas is through the plasma pressure in the momentum equation. The generalized MHD model for core plasma includes core ion FLR effects which provide a finite parallel electric field, a modified perpendicular velocity from the  $\mathbf{E} \times \mathbf{B}$  drift, and a gyroviscosity tensor, all of which are neglected in the usual single fluid MHD description. The perturbed core plasma electron and ion densities, velocity and pressure tensor (consisting of the diagonal pressure and gyroviscosity) are determined from both the low frequency and high frequency gyro-kinetic equations. From the quasineutrality condition, we obtain the parallel electric field, which arises from the ion gyroradius effects due to ion inertia (or ion mass) and the parallel electron inertia effect. Both

the perpendicular fluid velocity and the gyroviscosity tensor contains both core ion FLR and  $\omega/\omega_{ci}$  corrections. The kinetic-MHD model is closed by generalized pressure laws for both the core and energetic plasmas. When ion gyroradius radius is on the order of the plasma equilibrium scale length such as in a very thin magnetotail, the Vlasov description may be adopted to describe the energetic particle dynamics. From the kinetic-MHD model we derive the kinetic-MHD eigenmode equations for low frequency waves such as shear/kinetic Alfvén waves (KAW) and ballooning-mirror modes. The kinetic-MHD model has been successfully applied to study ballooning-mirror instabilities to understand the field-aligned structure and instability threshold of compressional Pc 5 waves in the ring current region. It is also demonstrated that the ion FLR effects in the dispersion relation of KAWs are properly retained. Note that the ion FLR effects are not properly included in the popularly employed two-fluid equations because the gyroviscosity contribution is usually not retained.

## I. INTRODUCTION

One of the grand challenges in space plasma physics is to study low frequency multiscale kinetic-MHD phenomena in which kinetic physics involving small spatial and fast temporal scales can strongly affect the global structure and long time behavior of space plasmas. Coupling between multiple spatial and temporal scales is an inherently difficult process to model. The difficulty stems from the disparate scales which traditionally are analyzed separately. Long time global-scale phenomena are generally studied using the single fluid MHD framework, while short time microscale phenomena are best described with kinetic theories.

The single fluid MHD model treats the plasma as a conducting fluid and its major advantage is that the governing equations are much simpler than the kinetic equations and

properly describe the global geometrical effects. The basic assumption of the ideal MHD model is that the plasma is frozen in the field line and moves with the  $\mathbf{E} \times \mathbf{B}$  drift, and the parallel electric field is zero. In the resistive MHD limit the parallel electric field is proportional to the parallel current density through plasma resistivity. The plasma pressure follows the adiabatic pressure law through plasma convection as well as compression. The fundamental shortcomings of the MHD model are that (a) the magnetic drift velocity is assumed to be small in comparison with the  $\mathbf{E} \times \mathbf{B}$  drift velocity and (b) kinetic effects such as finite particle Larmor radius, wave-particle resonances and particle trapping in a nonuniform magnetic field are ignored. Therefore, the basic assumptions of the MHD model can become invalid when particle kinetic effects are important. For example, energetic particles can significantly affect the MHD stability because their kinetic effects are vitally important due to high energy. For low frequency MHD modes with  $\omega \ll \omega_d$ , where  $\omega_d$  is the particle magnetic drift frequency and is proportional to the particle energy, the energetic particle dynamics are no longer governed by the  $\mathbf{E} \times \mathbf{B}$  drift, but rather by the magnetic ( $\nabla B$  and curvature) drift because the particle magnetic drift velocity is proportional to the particle energy. For the shear Alfvén waves with  $\omega \simeq \omega_b + \omega_d$  ( $\omega_b$  is the energetic trapped particle bounce frequency), the MHD shear Alfvén modes can be driven unstable by energetic particles resonating with the background waves because  $\omega_b$  is proportional to the particle velocity. In addition, kinetic Alfvén waves with perpendicular wavelength on the order of ion gyroradii can arise because ions do not move with the field lines as electrons. The resultant charge separation not only allows the kinetic Alfvén waves to travel across the field lines but also gives rise to a parallel electric field. Because the particle gyroradius is proportional to the particle velocity, energetic ions resonating with the kinetic Alfvén waves can decouple from the magnetic fields and lead to an effective diffusion across the magnetic field. In addition, the parallel electric field can effectively accelerate or decelerate resonant ions.

To take advantage of the simplicity of the MHD model and to properly take into account major kinetic effects of energetic particles, we have previously developed a kinetic-MHD

model [1]. In space environment the plasma can be considered to consist of two components: (1) a low energy core component which has major density fraction and (2) an energetic component which has low density, high energy and high  $\beta$ , and does not satisfy the MHD description. Each component can consist of more than one particle species. Instead of employing a full kinetic approach for all particle species, the kinetic-MHD model treats the low energy core plasma by the ideal MHD description and energetic particles by a kinetic approach such as the gyrokinetic equation [2] or Vlasov equation. The coupling between the dynamics of these two components of plasmas is through the plasma pressure in the momentum equation. Because the plasma resistivity and kinetic effects of the core component are neglected, the parallel electric field vanishes. The kinetic-MHD model optimizes both the physics content and the theoretical (analytical as well as numerical) effort, and properly accounts for the dynamics of high- $\beta$  plasma with pressure anisotropy in general magnetic field geometries. It is convenient for studying low frequency MHD type instabilities, wave propagation, and associated energetic particle transport.

The major weakness of the previously developed kinetic-MHD model [1] is that the kinetic effects associated with core plasma component are neglected. The core plasma kinetic effects modify the Ohm's law and introduces a gyroviscosity stress tensor to the momentum equation, and modifies the adiabatic pressure law. In the past reduced fluid models with ion FLR effects have been developed for low  $\beta$  plasmas [3]. In this paper we shall introduce the core ion finite Larmor radius (FLR) effects in our kinetic-MHD model [1] for high  $\beta$  plasmas with a minimum of modification by developing a generalized one-fluid MHD model that includes the parallel electric field and FLR effects in perpendicular velocity and gyroviscosity tensor with the assumptions that  $k_{\parallel} < k_{\perp}$ ,  $k_{\perp}^2 \rho_i^2 < 1$  and  $\omega_{ci}, k_{\parallel} v_e > \omega > k_{\parallel} v_i, \omega_{de,i}$ . The derivation of the generalized one-fluid MHD equations is based on a general frequency gyrokinetic model [2,4]. The perturbed core plasma density, velocity and pressure tensor are determined from the gyro-kinetic equation. From the quasineutrality condition, we obtain the parallel electric field, which arises from the ion polarization drift and parallel electron inertia effects. Thus, the generalized Ohm's law contains core ion FLR effects on

the parallel electric field and the perpendicular fluid velocity. The generalized one-fluid model for the core plasma component can be combined with a kinetic description (such as the gyrokinetic equation or Vlasov equation) for the energetic particle component to form a kinetic-MHD model that couples between the dynamics of these two components of plasmas through the plasma pressure in the momentum equation.

In Sec. II we will review a kinetic-MHD model that incorporates energetic particle kinetic effects. In Sec. III we demonstrate that the kinetic-MHD model can be successfully applied to study ballooning-mirror instabilities to understand the field-aligned structure and instability threshold of compressional Pc 5 waves in the ring current region. Then, in Sec IV we present a generalized kinetic-MHD model that also includes core ion finite ion Larmor radius (FLR) effects. We will show that the generalized kinetic-MHD model properly retains the ion FLR effects in the parallel electric field, perpendicular velocity and gyroviscosity tensor. Then, in Sec V we present kinetic-MHD eigenmode equations for low frequency kinetic-MHD modes including both core ion FLR and energetic particle kinetic effects. In particular, the dispersion relations of ballooning-mirror modes and kinetic Alfvén waves (KAW) are given. Finally a summary and discussion is given in Sec. VI.

## II. A KINETIC-MHD MODEL INCORPORATING ENERGETIC PARTICLE KINETIC EFFECTS

To incorporate energetic particle kinetic effects into MHD formulation we had previously developed a hybrid kinetic-MHD model [1] for describing low-frequency phenomena in high  $\beta$  ( $\beta \simeq O(1)$ ) anisotropic plasmas that consist of two components: a low energy core ( $c$ ) background component and an hot ( $h$ ) component with low density so that  $n_h \ll n_c$ , and  $T_h \gg T_c$ . The kinetic-MHD model treats the low energy core component by ideal MHD description, the energetic component by kinetic approach such as the gyrokinetic equation, and the coupling between the dynamics of these two components through plasma pressure in the momentum equation. The kinetic-MHD model is applicable to magnetized collisionless

plasma system where the parallel electric field effects are negligibly small.

Because the plasma usually has anisotropic pressure in space environment and large magnetic fusion devices, we consider the momentum equation with anisotropic pressure

$$\rho \frac{d}{dt} \mathbf{V} = -\nabla \cdot \mathbf{P} + \mathbf{J} \times \mathbf{B}, \quad (1)$$

where  $(d/dt) = (\partial/\partial t) + \mathbf{V} \cdot \nabla$  is the total time derivative,  $\mathbf{V}$  is the fluid velocity,  $\mathbf{B}$  is the magnetic field,  $\mathbf{P}$  is the pressure tensor due to all particle species, and  $\rho$  is the total plasma mass density. The density continuity equation is given by  $d\rho/dt + \rho \nabla \cdot \mathbf{V} = 0$ . The Ohm's law is given by  $\mathbf{E} + \mathbf{V} \times \mathbf{B} = \eta \mathbf{J}$ , where  $\mathbf{E}$  is the electric field and  $\eta$  is the plasma resistivity. The Maxwell's equations hold: the Faraday's law,  $\partial \mathbf{B} / \partial t = -\nabla \times \mathbf{E}$ ; the Ampere's law,  $\mathbf{J} = \nabla \times \mathbf{B}$ ; and  $\nabla \cdot \mathbf{B} = 0$ . The total plasma pressure can be expressed as  $\mathbf{P} = P_{\perp} \mathbf{I} + (P_{\parallel} - P_{\perp}) \mathbf{B} \mathbf{B} / B^2$ , where  $P_{\parallel}$  and  $P_{\perp}$  are the parallel and perpendicular pressures, respectively, and contain both the core and hot plasma pressures. To close the above equations we need to prescribe the pressure. Because the hot plasma density is much smaller than the core plasma density we employ the double-adiabatic pressure laws to relate the core plasma pressure to the plasma density;

$$\frac{d}{dt} \left( \frac{P_{\parallel c} P_{\perp c}^2}{\rho^5} \right) = 0 \quad (2)$$

and

$$\frac{d}{dt} \left( \frac{P_{\perp c}}{\rho B} \right) = 0. \quad (3)$$

For the hot component we account for particle kinetic effects, such as finite Larmor radius and wave-particle resonances, by obtaining the parallel and perpendicular pressures from the hot particle distribution function  $f$  by

$$\begin{aligned} P_{\parallel h} &= \sum_j m_j \int d^3v v_{\parallel}^2 f_j \\ P_{\perp h} &= \sum_j \frac{m_j}{2} \int d^3v v_{\perp}^2 f_j \end{aligned} \quad (4)$$

where the summation in  $j$  is over all hot particle species,  $m$  is the particle mass, and  $v_{\parallel}$  and  $v_{\perp}$  are the particle velocity parallel and perpendicular to the magnetic field  $\mathbf{B}$ , respectively.

The low-frequency gyrokinetic formulation is employed to describe the dynamics of all hot particle species. We consider waves with  $\omega \ll \omega_{ci}$ ,  $k_{\perp} > k_{\parallel}$  and assume a WKB eikonal representation for perturbed quantities, *i.e.*,  $\delta f(\mathbf{x}, \mathbf{v}, t) = \delta f(s, \mathbf{k}_{\perp}, \mathbf{v}, t) \exp(i \int d\mathbf{x}_{\perp} \cdot \mathbf{k}_{\perp})$ , where  $s$  is the distance along the equilibrium magnetic field. The perturbed particle distribution function for a given species is written as

$$\delta f = \frac{q}{m} \frac{\partial F}{\partial \mathcal{E}} \Phi + \frac{q}{mB} \frac{\partial F}{\partial \mu} (\Phi - v_{\parallel} A_{\parallel}) + [g_0 - \frac{q}{mB} \frac{\partial F}{\partial \mu} \langle \delta L \rangle] \exp(iL_0), \quad (5)$$

where  $F$  is the equilibrium particle distribution function,  $\langle \delta L \rangle = (\Phi - v_{\parallel} A_{\parallel}) J_0(k_{\perp} v_{\perp} / \omega_c) + (v_{\perp} \delta B_{\parallel} / k_{\perp}) J_1(k_{\perp} v_{\perp} / \omega_c)$ ,  $L_0 = (\mathbf{k}_{\perp} \times \mathbf{v}_{\perp} \cdot \mathbf{B}) / \omega_c B$ ,  $\mathcal{E} = v^2 / 2$ ,  $\mu = v_{\perp}^2 / 2B$ ,  $q$  is the particle charge,  $\omega_c = qB / mc$ , and  $\Phi$ ,  $A_{\parallel}$ , and  $\delta B_{\parallel}$  are the electrostatic potential, vector potential and perturbed magnetic field parallel to the equilibrium magnetic field  $\mathbf{B}$ , respectively.  $J_0$  and  $J_1$  are the Bessel functions of order 0 and 1, respectively. The nonadiabatic particle distribution  $g_0$  is governed by the nonlinear gyrokinetic equation [2]

$$\left[ \frac{\partial}{\partial t} + (\mathbf{v}_{\parallel} + \mathbf{v}_d) \cdot \nabla \right] g_0 = - \left[ \frac{q}{m} \frac{\partial F}{\partial \mathcal{E}} \frac{\partial}{\partial t} - \frac{\mathbf{B} \times \nabla (F + g_0)}{B^2} \cdot \nabla \right] \langle \delta L \rangle, \quad (6)$$

where  $\mathbf{v}_d = (\mathbf{B} / B \omega_c) \times [\nabla(\mu B) + \boldsymbol{\kappa} v_{\parallel}^2]$  is the particle magnetic drift velocity,  $\boldsymbol{\kappa} = \hat{\mathbf{b}} \cdot \nabla \hat{\mathbf{b}}$  is the magnetic field curvature, and  $\hat{\mathbf{b}} = \mathbf{B} / B$ .

Equations (1)-(6) form the basis of the gyrokinetic-MHD model that includes dominant energetic particle kinetic effects. When more accurate solution of  $\delta f$  is required, such as in the magnetotail region where the particle Larmor radius is comparable to the equilibrium scale length, the Vlasov equation must be employed to solve  $\delta f$  in order to couple to the MHD fluid equations.

### III. BALLOONING-MIRROR INSTABILITIES IN THE RING CURRENT

The kinetic-MHD model has been successfully applied to study linear MHD instabilities in the ring current region. In particular, the ballooning-mirror instabilities have been identified to be responsible for the internally driven compressional Pc 5 waves [5-7]. Internally

driven compressional Pc 5 waves usually have large azimuthal mode numbers (on the order of 100) and are usually observed around the Earth's magnetic equator in the ring current region by satellites [8] during periods of enhanced ring current intensity and are associated with high- $\beta$ , anisotropic pressure plasmas with  $P_{\perp} > P_{\parallel}$ . Multi-satellite observation of compressional Pc 5 wave events [8–10] revealed that the field-aligned structure of the compressional magnetic field,  $\delta B_{\parallel}$ , is antisymmetric with respect to the Earth's magnetic equator as shown in Fig. 1. The smaller transverse magnetic components (radial component,  $\delta B_r$ , and azimuthal component,  $\delta B_{\phi}$ ) have a symmetric parity and their polarization varies with the magnetic latitude. The wave frequencies are about one order of magnitude smaller than the shear Alfvén frequency obtained from the measured plasma density and wave structures along the ambient magnetic field.

To understand the internally driven compressional Pc 5 waves we have applied the kinetic-MHD model to study the ballooning-mirror instabilities [1, 5, 6] in the magnetospheric ring current region, where the plasma pressure is mainly contributed by ions with energy larger than 1 keV, but the plasma mass density is mainly due to core thermal ions with energy less than 1 keV. Based on the kinetic-MHD model, two coupled field-aligned kinetic-MHD eigenmode equations have been derived to describe coupling between the transverse and the compressional magnetic field components with large azimuthal mode numbers [1]. The compressional magnetic field equation is given by

$$\mathbf{B} \cdot \nabla \left( \frac{\sigma}{B^2} \mathbf{B} \cdot \nabla \delta B_{\parallel} \right) + \frac{\rho \omega^2}{B^2} \delta B_{\parallel} - k_{\perp}^2 \left[ \tau \delta B_{\parallel} - \frac{\mathbf{B} \times \tilde{\nabla} P_{\perp} \cdot \mathbf{k}_{\perp}}{B^3} \hat{\Phi} + \frac{\delta \hat{P}_{\perp}}{B} \right] = 0, \quad (7)$$

where  $\hat{\Phi} (= \Phi/\omega)$ ,  $\sigma = 1 + (P_{\perp} - P_{\parallel})/B^2$ ,  $\tau = 1 + (1/B)(\partial P_{\perp}/\partial B)_{\psi}$ , and  $\tilde{\nabla} = \nabla - \nabla B(\partial/\partial B)_{\psi}$ , and the subscript  $\psi$  represents the poloidal magnetic flux of a L-shell magnetic surface. Equation (7) indicates that the mirror mode can be destabilized by the combined effect of plasma  $\beta$  and pressure anisotropy with  $P_{\perp} > P_{\parallel}$ . In ideal MHD limit, mirror modes are unstable for  $\tau < 0$ . The transverse magnetic field equation

$$\begin{aligned} \mathbf{B} \cdot \nabla \left( \frac{\sigma k_{\perp}^2}{B^2} \mathbf{B} \cdot \nabla \hat{\Phi} \right) + \frac{\rho k_{\perp}^2 \omega^2}{B^2} \hat{\Phi} \\ + \frac{\mathbf{B} \times \boldsymbol{\kappa} \cdot \mathbf{k}_{\perp}}{B^2} \left[ \frac{\mathbf{B} \times \tilde{\nabla} P_{\parallel}}{B^2} \cdot \mathbf{k}_{\perp} \hat{\Phi} + \sigma B \delta B_{\parallel} - \delta \hat{P}_{\parallel} \right] = 0. \end{aligned} \quad (8)$$

In ideal MHD limit, the necessary condition is  $\boldsymbol{\kappa} \cdot \nabla P > 0$  for unstable ballooning modes and is  $\sigma < 0$  for the fire hose instability. Note that kinetic effects due to hot trapped particles are included in the nonadiabatic perturbed pressures  $\delta \hat{P}_{\perp}$  and  $\delta \hat{P}_{\parallel}$ , which are given by

$$\begin{pmatrix} \delta \hat{P}_{\parallel} \\ \delta \hat{P}_{\perp} \end{pmatrix} = \sum_j m \int d^3v g_0 \begin{pmatrix} 2(\varepsilon - \mu B) \\ \mu B \end{pmatrix}. \quad (9)$$

Equation (8) describes the ballooning mode which can be destabilized by the combined effect of the magnetic field curvature and the plasma pressure gradient. The coupling between the compressional and transverse magnetic field components, which determines the stability of the ballooning-mirror instabilities, is due to finite perpendicular pressure gradient and the perturbed kinetic particle pressures.

Kinetic effects in  $\delta \hat{P}_{\parallel}$  and  $\delta \hat{P}_{\perp}$  are associated with energetic trapped particles and play an essential role in determining the stability and structure of the ballooning-mirror mode. Without the hot particle kinetic effects MHD modes with symmetric structure of parallel perturbed magnetic field,  $\delta B_{\parallel}$ , and electrostatic potential,  $\Phi$ , along the north-south ambient magnetic field would be more unstable than the antisymmetric mode. However, if energetic trapped particle kinetic effects are included, the symmetric ballooning-mirror mode can be completely stabilized. This process can be understood by considering the particle dynamics in a MHD perturbation. If the ballooning-mirror instability frequency is smaller than the energetic trapped particle magnetic drift frequency (which is much smaller than the bounce frequency) energetic trapped particles experience a finite bounce-averaged wave structure and their kinetic pressure response from  $\delta \hat{P}_{\parallel}$  and  $\delta \hat{P}_{\perp}$  cancels with their fluid pressure response so that the symmetric mode is stabilized. The mathematical proof was given in the paper by [6]. Physically, the energetic trapped particles precess rapidly across the magnetic field, and their motion becomes rigid with respect to low frequency symmetric

MHD perturbations.

However, for antisymmetric modes the energetic trapped particle kinetic pressure response from the northern hemisphere cancels with that from the southern hemisphere in a bounce period so that both  $\delta\hat{P}_{\parallel}$  and  $\delta\hat{P}_{\perp}$  vanish, and the instability  $\beta$  threshold is determined by the energetic particle fluid free energy. For  $(P_{\perp}/P_{\parallel}) \geq (1 + 1/\beta_{\perp})$ , the field-aligned structure of the antisymmetric ballooning-mirror instability agrees with the multi-satellite observation of compressional Pc 5 wave structure [8–10]. In Fig. 1 we present a comparison of the field-aligned structure of the perturbed magnetic field between a theoretical solution of an antisymmetric ballooning-mirror mode and the multi-satellite (SCATHA, GOES 2, GOES 3, GEOS 2) observation of a long lasting compressional Pc 5 wave event during November 14-15, 1979 [9, 10]. The numerical solution was obtained for bi-Maxwellian plasmas in a dipole magnetic field with the equatorial parameters:  $P_{\perp}/P_{\parallel} = 2$ ,  $\beta_{\parallel} = 0.575$  ( $\tau = -0.149$ ),  $\partial \ln P / \partial \ln L = -5$ , and  $L = 6.6$ . The agreement between the observation and our theory strongly suggests that this particular multi-satellite observation is related to marginally unstable ballooning-mirror modes with  $\tau$  value close to zero, where  $\tau = 1 + \beta_{\perp}(1 - P_{\perp}/P_{\parallel})$ .

Figure 2 shows the theoretical stability boundaries of the antisymmetric ballooning-mirror modes for different  $\partial \ln P / \partial \ln L$  values in the equatorial  $(\tau, \alpha_p)$  space, where  $\alpha_p$  represent the ballooning instability parameter and is given by

$$\alpha_p = \frac{k_{\phi}^2}{k_{\perp}^2}(\kappa_c L) \left[ \frac{\sigma P_{\perp}}{\tau B^2} \frac{\partial \ln P_{\perp}}{\partial \ln L} + \frac{P_{\parallel}}{B^2} \frac{\partial \ln P_{\parallel}}{\partial \ln L} \right], \quad (10)$$

where  $\kappa_c$  is the normal magnetic field curvature across the L-shell. Note that  $\alpha_p$  and  $\tau$  are not linearly independent and for  $\tau < 0$  the  $\alpha_p$  threshold is also negative, and we have plotted absolute value of  $\alpha_p$  in Fig. 2 for  $\tau < 0$ . Above the marginal stability boundary curves the antisymmetric ballooning-mirror modes are unstable. The marginal stability boundary curves in the equatorial  $(\tau, \alpha_p)$  space are very close to each other even for  $100 > \partial \ln P / \partial \ln L > 1$ . This probably holds even for different type of particle velocity distributions. This property is useful when we compare theoretical calculations with satellite observations where information on  $\partial \ln P / \partial \ln L$  and particle velocity distribution either is unavailable or cannot

## Field-Aligned Structure of Perturbed Magnetic Field

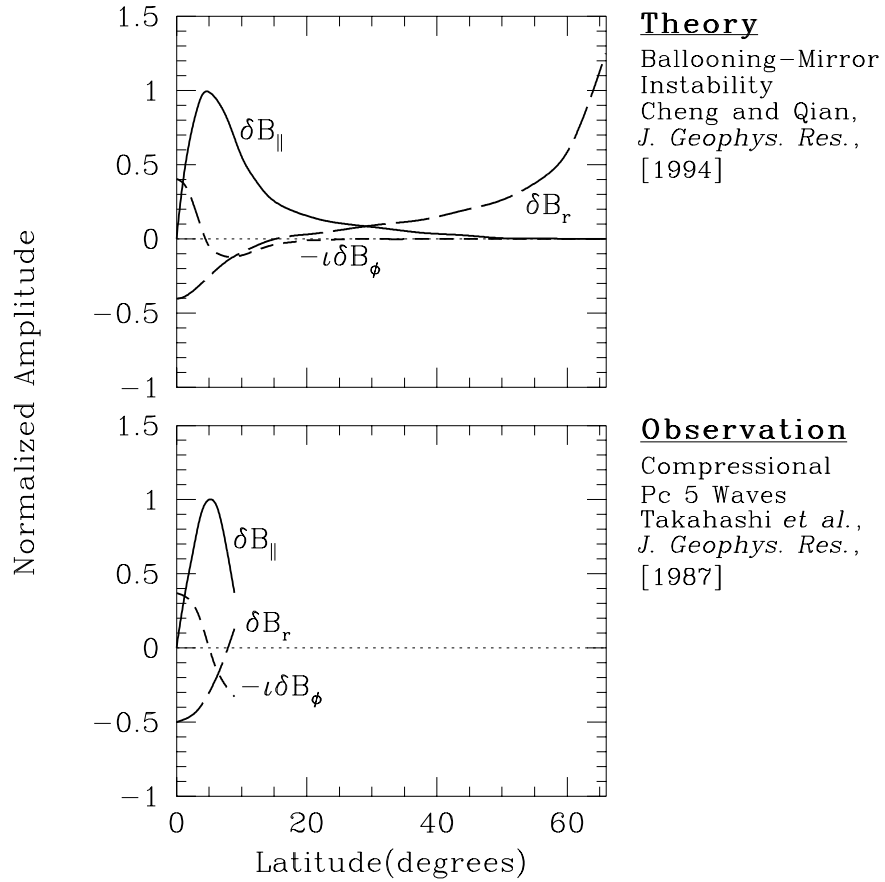


FIG. 1. A comparison of the field-aligned structure of the perturbed magnetic field between a theoretical solution of an antisymmetric ballooning-mirror mode and the multi-satellite (SCATHA, GOES 2, GOES 3, GEOS 2) observation of a long lasting compressional Pc 5 wave event during November 14-15, 1979.

be obtained accurately. To test the theoretical antisymmetric ballooning-mirror instability threshold against observations we have computed values of  $\tau$  and  $\alpha_p$  from the AMPTE/CCE particle data acquired with the ion charge-energy-mass spectrometer (CHEM) for 10 Pc 4-5 wave events [7]. In Fig. 2 we also plotted the “observed” values of  $\tau$  and  $\alpha_p$  against the theoretical stability threshold. The symbol “O” represents compressional wave events and the symbol “+” represents transverse wave events. When there is no wave activity the values of  $\tau$  and  $\alpha_p$  tend to be well below the antisymmetric ballooning-mirror instability thresholds. The transverse and compressional wave events clearly occupy different domains in the  $(\tau, \alpha_p)$  space. For compressional wave events the values of  $\tau$  and  $\alpha_p$  are either near or above the theoretical stability boundary curves of the antisymmetric ballooning-mirror modes with  $\tau \leq 0.6$  and  $O(10) \leq \alpha_p \leq O(10^3)$ . The transverse waves tend to occur when  $\tau$  is close to unity and  $1 \leq \alpha_p \leq O(10)$ , which are at least one order of magnitude below the theoretical antisymmetric ballooning-mirror instability threshold.

Therefore, we have demonstrated that internally driven compressional Pc 5 waves are caused by antisymmetric ballooning-mirror modes and can be successfully studied by our kinetic-MHD model [1]. They represent genuine multiscale kinetic-MHD phenomena; fast time scale trapped particle motion strongly couples to slow time scale MHD modes. We emphasize that the ideal MHD theory predicts an opposite result from our kinetic-MHD theory which is in close agreement with the observations.

#### **IV. A GENERALIZED MHD MODEL INCORPORATING CORE ION FINITE LARMOR RADIUS EFFECTS**

The previously developed kinetic-MHD model [1] retains kinetic effects of the energetic particle component, but neglects kinetic effects of the core thermal plasma component. However, for phenomena such as kinetic Alfvén waves core ion finite Larmor radius effects and plasma dissipations through wave-particle resonances need to be included. Kinetic Alfvén waves have been proposed as a possible candidate for causing plasma transport across

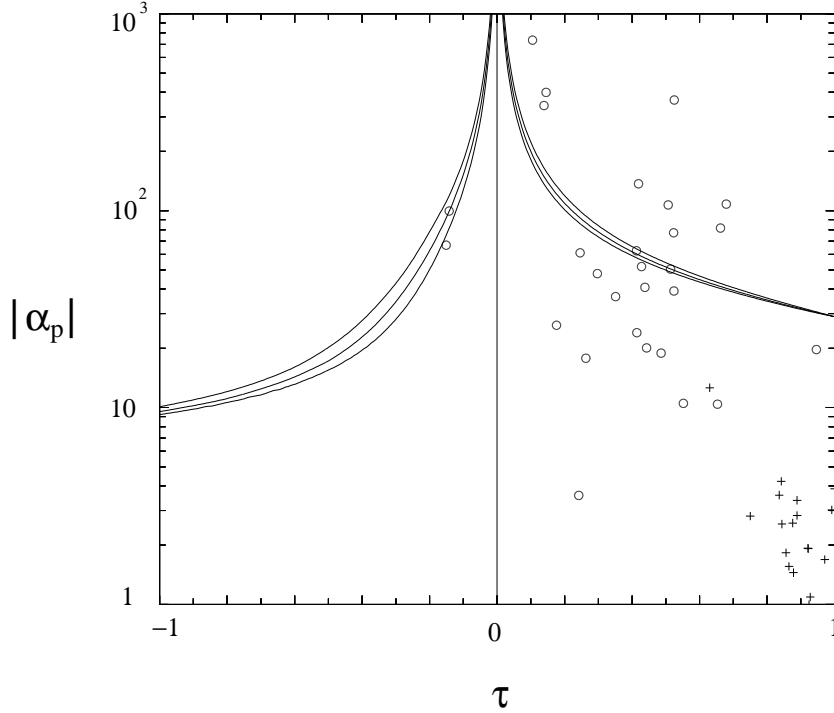


FIG. 2. A comparison of the theoretical stability boundaries of the antisymmetric ballooning-mirror modes for different  $\partial \ln P / \partial \ln L$  values in the equatorial  $(\tau, \alpha_p)$  space against “observed” values computed from the AMPTE/CCE particle data acquired with the ion charge-energy-mass spectrometer (CHEM) for 10 Pc 4-5 compressional and transverse wave events.

the magnetopause [11,12]. Ion kinetic effects are also important in MHD wave activity during substorms [13]. In this section we refine the kinetic-MHD model to include the core ion finite Larmor radius effects. The effects of core ion wave-particle resonances will be studied in the future.

To retain core ion FLR effects, we develop a generalized MHD model based on kinetic description of the particle distribution functions. The ion FLR effects result from the ion gyromotion motion due to finite ion mass inertia so that its perpendicular motion deviates from the  $\mathbf{E} \times \mathbf{B}$  drift. Charge separation resulting from different motion between electrons and ions due to ion FLR effects causes a finite parallel electric field. Thus the ion FLR effects provide a modified Ohm’s law. In addition, the ion FLR effects also introduce a gyroviscous force in the momentum equation.

To properly take into account ion FLR effects based on the gyrokinetic formulation, we need to include finite  $\omega/\omega_{ci}$  correction to the gyrokinetic particle distribution function. We adopt a general frequency gyrokinetic formulation [4] with the perturbed particle distribution function expressed as

$$\begin{aligned} \delta f = & \frac{q}{m} \frac{\partial F}{\partial \mathcal{E}} \Phi + \frac{q}{mB} \frac{\partial F}{\partial \mu} (\Phi - v_{\parallel} A_{\parallel}) \\ & + \sum_l \left\{ g_l - \frac{q}{mB} \frac{\partial F}{\partial \mu} [(\Phi - v_{\parallel} A_{\parallel}) J_l - \frac{v_{\perp} \delta B_{\parallel}}{k_{\perp}} J'_l] \right\} \exp(iL_l), \end{aligned} \quad (11)$$

where  $L_l = \mathbf{k}_{\perp} \times \mathbf{v}_{\perp} \cdot \hat{\mathbf{b}}/\omega_c - l\theta$ ,  $\theta$  is the particle gyrophase angle between  $\mathbf{k}_{\perp}$  and  $\mathbf{v}_{\perp}$ ,  $g_l$  is the nonadiabatic contribution to the particle distribution function, and  $J_l$  is the Bessel function of order  $l$  with argument  $k_{\perp} v_{\perp}/\omega_{ci}$ . For  $l = 0$ ,  $g_l$  represents the main low frequency contribution for  $\omega < \omega_{ci}$  and is governed by the nonlinear gyrokinetic equation, Eq. (6) [2]. For  $l \neq 0$ ,  $g_l$  represents the  $(\omega/\omega_{ci})$  correction to the particle distribution function. Because we are interested in low frequency phenomena the nonlinear effects in  $g_l$  can be ignored. Then,  $g_l$  is governed by the linearized general frequency gyrokinetic equation [4]

$$(\omega + iv_{\parallel} \frac{\partial}{\partial s} - \omega_d - l\omega_c) g_l = \frac{qF}{T} (\tilde{\omega}_l - \omega_*^T) [(\Phi - v_{\parallel} A_{\parallel}) J_l - \frac{v_{\perp} \delta B_{\parallel}}{k_{\perp}} J'_l], \quad (12)$$

where  $\tilde{\omega}_l = -T/m[\omega \partial/\partial \mathcal{E} + (l\omega_c/B) \partial/\partial \mu] \ln F$ , and  $\omega_*^T = (T/qB) \mathbf{k}_{\perp} \cdot \hat{\mathbf{b}} \times \nabla \ln F$ . Finite Larmor radius effects are included through the Bessel functions, and the theoretical framework is valid even for  $k_{\perp} \rho_i = O(1)$ .

In the following we will present generalized MHD equations obtained from approximate solutions of the gyrokinetic equation by taking the frequency ordering:  $\omega_{ci}, k_{\parallel} v_e > \omega > k_{\parallel} v_i, \omega_{*e,i}, \omega_{de,i}$  ( $\omega_d = \mathbf{k} \cdot \mathbf{v}_d$ ) and the spatial scale ordering:  $k_{\parallel}^{-1} > k_{\perp}^{-1} > \rho_i$ . In particular, we shall retain the leading order contribution in  $(\omega/\omega_{ci})$  and  $(k_{\perp}^2 \rho_i^2)$ , but ignore diamagnetic and magnetic drift effects as well as dissipative effects associated with wave-particle resonances.

Because the hot particle density is assumed to be small in comparison with core plasma density, the parallel electric field is determined from the quasineutrality condition and is given by

$$\mathbf{E}_{\parallel} \simeq \sum_i \frac{n_i q_i^2 T_{\parallel e}}{n_e q_e^2} \nabla_{\parallel} \left( \frac{\nabla_{\perp} \cdot \mathbf{E}_{\perp}}{m_i \omega_{ci}^2} - \frac{P_{\perp i}}{P_{\parallel i}} \frac{\delta B_{\parallel}}{q_i B} \right), \quad (13)$$

where the summation is over all core ion species. In obtaining Eq. (13) we have assumed the electron pressure to be isotropic. Physically the  $\nabla_{\perp} \cdot \mathbf{E}_{\perp}$  term is due to ion gyromotion, but is proportional to the electron temperature due to fast electron motion along the field line that maintains charge quasineutrality. The  $\delta B_{\parallel}$  term is related to the divergence of the slow ion parallel fluid motion. In the ionosphere the electron inertia effect should be included due to small ion Larmor radius and the parallel electric field for low  $\beta$  plasma is given by

$$\mathbf{E}_{\parallel} \approx \left[ \left( \sum_i \frac{n_i q_i^2}{n_e q_e^2} \frac{T_{\parallel e}}{m_i \omega_{ci}^2} - \lambda_e^2 \right) / \left( 1 + k_{\perp}^2 \lambda_e^2 \right) \right] \nabla_{\parallel} \nabla_{\perp} \cdot \mathbf{E}_{\perp}, \quad (14)$$

where  $\lambda_e = c/\omega_{pe}$  is the electron skin depth, and the diamagnetic drift effects are small and can be ignored in the ionosphere. For magnetospheric conditions the parallel electric field is dominated by finite ion Larmor radius effects because  $T_{\parallel e}/m_i \omega_{ci}^2 \gg \lambda_e^2$ .

Because the electron perpendicular velocity is mainly the  $\mathbf{V}_E$  drift velocity, where  $\mathbf{V}_E = \mathbf{E} \times \mathbf{B}/B^2$ , the perpendicular fluid velocity can be well approximated by the ion perpendicular velocity. From the velocity moment of the ion distribution the perpendicular fluid velocity is determined by

$$\rho \mathbf{V}_{\perp} \simeq \sum_i n_i m_i \left[ \left( 1 + \frac{3 P_{\perp i} \nabla_{\perp}^2}{2 n_i m_i \omega_{ci}^2} \right) \mathbf{V}_E + \frac{2 P_{\perp i} \mathbf{B} \times \nabla \delta B_{\parallel}}{q_i n_i B^3} + \frac{1}{B \omega_{ci}} \frac{\partial \mathbf{E}_{\perp}}{\partial t} \right]. \quad (15)$$

On the right hand side of the above equation the first term in the first square bracket is related to the  $\mathbf{V}_E$  drift with finite ion Larmor radius correction, the second term is related to the  $\nabla B$  drift associated with the perturbed magnetic field. and the third term is due to the polarization drift which is usually small and is on the order of  $\omega/\omega_{ci}$ . Note that the ion diamagnetic drift correction is also retained. Equations (13) and (15) form the generalized Ohm's law which relates the electric field to the fluid velocity. The generalized Ohm's law includes effects associated with leading finite ion Larmor radius and finite  $\omega/\omega_{ci}$  corrections.

Next, we write the pressure tensor as  $\mathbf{P} = \mathbf{P}_{CGL} + \mathbf{\Pi}_g$ , where  $\mathbf{P}_{CGL} = P_{\perp} \mathbf{I} + (P_{\parallel} - P_{\perp}) \hat{\mathbf{b}} \hat{\mathbf{b}}$  is the Chew-Goldberger-Low pressure tensor and  $\mathbf{\Pi}_g$  is the gyroviscous stress tensor. The gyroviscous force is mainly contributed by finite ion Larmor radius effects and is given by

$$\nabla \cdot \mathbf{\Pi}_g \simeq \nabla_{\perp} \Lambda - \sum_i \frac{\partial}{\partial t} \left[ \frac{3 P_{\perp i} \nabla_{\perp}^2}{4 \omega_{ci}^2} \mathbf{V}_E + \frac{P_{\perp i}}{2 \omega_{ci} B^2} \mathbf{B} \times \nabla \delta B_{\parallel} \right], \quad (16)$$

and  $\Lambda$  is given by

$$\Lambda \simeq - \sum_i \frac{q_i P_{\perp i} \nabla_{\perp} \cdot \mathbf{E}_{\perp}}{2m_i \omega_{ci}^2}. \quad (17)$$

Note that the second term on the right hand side of Eq. (16) is due to finite  $\omega/\omega_{ci}$  frequency correction and thus, the  $l \neq 0$  terms must be retained in the gyrokinetic equations, Eqs. (11) and (12). Also note that the gyroviscous force must be included to obtain the kinetic Alfvén wave dispersion relation with proper finite Larmor radius effects.

To close the fluid equations we need to determine the dynamics of the CGL pressures of core particle species. The equations for CGL pressures of core particle species can be similarly derived from the gyrokinetic equations and for ions they are given by

$$\left( \frac{\partial}{\partial t} + \mathbf{V}_E \cdot \nabla \right) P_{\perp i} = -2P_{\perp i} \left( \frac{\partial}{\partial t} + \mathbf{V}_E \cdot \nabla \right) \left( \frac{q_i \nabla_{\perp} \cdot \mathbf{E}_{\perp}}{m_i \omega_{ci}^2} - \frac{\delta B_{\parallel}}{B} \right), \quad (18)$$

and

$$\left( \frac{\partial}{\partial t} + \mathbf{V}_E \cdot \nabla \right) P_{\parallel i} = -P_{\parallel i} \left( \frac{\partial}{\partial t} + \mathbf{V}_E \cdot \nabla \right) \left( \frac{q_i \nabla_{\perp} \cdot \mathbf{E}_{\perp}}{m_i \omega_{ci}^2} - \frac{\delta B_{\parallel}}{B} \right), \quad (19)$$

where the  $\nabla \cdot \mathbf{E}_{\perp}$  terms are related to ion FLR effect and the  $(\delta B_{\parallel}/B)$  terms are ion parallel motion that provides plasma compression. For electrons the pressure equations are given by

$$\left( \frac{\partial}{\partial t} + \mathbf{V}_E \cdot \nabla \right) P_{\perp e} = \frac{\partial}{\partial t} \left( n_e q_e \Psi + \frac{\partial P_{\perp e}}{\partial B} \delta B_{\parallel} \right), \quad (20)$$

and

$$\left( \frac{\partial}{\partial t} + \mathbf{V}_E \cdot \nabla \right) P_{\parallel e} = \frac{\partial}{\partial t} \left( n_e q_e \Psi + \frac{\partial P_{\parallel e}}{\partial B} \delta B_{\parallel} \right), \quad (21)$$

where  $\Psi$  is the parallel electric field potential defined by  $\mathbf{E}_{\parallel} = -\nabla_{\parallel} \Psi$ . Note from the quasineutrality relation, Eq. (13), that  $\Psi$  is on the order of  $(T_e/T_i)(k_{\perp}^2 \rho_i^2) \Phi$ , where  $\Phi$  is the electrostatic potential.

Thus, the generalized Ohm's law (Eqs. (13) and (15)), the generalized momentum equation (Eqs. (1) and (16)), the generalized pressure equations (Eqs. (18), (19)), (20) and (21)), and the mass density continuity equation constitute our proposed generalized MHD model.

Again, because wave-particle resonances can be important for hot particles their dynamics are described by the gyrokinetic equation and couple with the core plasma through the pressure force in the generalized momentum equation as in our previously proposed kinetic-MHD model [1].

## V. KINETIC-MHD EIGENMODE EQUATIONS INCORPORATING FLR EFFECTS

In order to show that our generalized MHD model provides proper core ion finite Larmor radius effects, we derive the linear kinetic-MHD eigenmode equations for describing low frequency kinetic-MHD waves with  $\omega \ll \omega_{ci}$ . In particular, the kinetic-MHD eigenmode equations should properly take into account the core ion FLR effects for kinetic Alfvén waves. We first rewrite the momentum equation into a more useful form

$$\rho \frac{d}{dt} \mathbf{V} = -\nabla(P_{\perp} + B^2/2) + \sigma \mathbf{B} \cdot \nabla \mathbf{B} + \mathbf{B}(\mathbf{B} \cdot \nabla \sigma) - \nabla \cdot \mathbf{\Pi}_g. \quad (22)$$

where  $\sigma = 1 + (P_{\perp} - P_{\parallel})/B^2$  and we have made use of the perpendicular equilibrium relation,  $\nabla_{\perp}(B^2/2 + P_{\perp}) = \kappa \sigma B^2$ . Note that  $\nabla(P_{\perp} + B^2/2)$  is the dominant term for perturbations with  $k_{\parallel} < k_{\perp}$ .

To retain the  $\nabla(P_{\perp} + B^2/2)$  term we apply the  $\mathbf{B} \cdot \nabla \times \mathbf{B} \times$  operator to the momentum equation, Eq. (22), and we obtain the linearized perpendicular current equation for  $\delta B_{\parallel}$

$$\begin{aligned} \mathbf{B} \cdot \nabla \left[ \frac{\sigma}{B^2} \mathbf{B} \cdot \nabla (\mathbf{B} \cdot \delta \mathbf{B}) \right] + \frac{\rho \omega^2}{B^2} \mathbf{B} \cdot \delta \mathbf{B} \\ + \nabla_{\perp}^2 \left( \delta P_{\perp} + \mathbf{B} \cdot \delta \mathbf{B} - \sum_i \frac{q_i P_{\perp i} \nabla_{\perp}^2 \Phi}{2m_i \omega_{ci}^2} \right) \simeq 0. \end{aligned} \quad (23)$$

Because the  $\mathbf{B} \times$  operator removes the parallel dynamics information Eq. (23) describes mainly waves associated with the compressional magnetic field. For  $\omega \ll k_{\perp} V_A$ , the perturbed perpendicular pressure is out of phase with the perturbed magnetic pressure.

To eliminate the  $\nabla(P_{\perp} + B^2/2)$  term we apply  $\mathbf{B} \cdot \nabla \times$  to the momentum equation, Eq. (22), and obtain the linearized parallel current (or vorticity) equation

$$\begin{aligned}
& B^2 \mathbf{B} \cdot \nabla \left[ \frac{\sigma \delta J_{\parallel}}{B} \right] - \mathbf{B} \times \boldsymbol{\kappa} \cdot \nabla (\mathbf{B} \cdot \delta \mathbf{B} - \delta P_{\parallel}) \\
& + \nabla \cdot \left( \rho \mathbf{B} \times \frac{\partial \mathbf{V}}{\partial t} \right) - \mathbf{B} \cdot \nabla \times (\nabla \cdot \boldsymbol{\Pi}_g) \simeq 0,
\end{aligned} \tag{24}$$

which represents the vanishing of the divergence of the current. From the perpendicular Ohm's law and the gyroviscous force expression we have

$$\begin{aligned}
& \nabla \cdot \left( \rho \mathbf{B} \times \frac{\partial \mathbf{V}}{\partial t} \right) - \mathbf{B} \cdot \nabla \times (\nabla \cdot \boldsymbol{\Pi}_g) \simeq \\
& + i \sum_i n_i m_i \omega \left[ \left( 1 + \frac{3 P_{\perp i} \nabla_{\perp}^2}{4 n_i m_i \omega_{ci}^2} \right) \nabla_{\perp}^2 \Phi + \frac{3 P_{\perp i}}{2 n_i m_i \omega_{ci}} \nabla_{\perp}^2 \delta B_{\parallel} \right].
\end{aligned} \tag{25}$$

Note that the core ion FLR effects enter mainly through the ion inertia term. Also note that for  $\beta_i \sim O(1)$  the  $\delta B_{\parallel}$  contribution resulting from the gyroviscous force is at least of the same order as the finite Larmor radius correction to the electrostatic potential.

From Eq. (23)  $\delta P_{\perp}$  is related to the compressional magnetic field, and from Eq. (24)  $\delta P_{\parallel}$  enters with the magnetic field curvature. To proceed, we shall assume that the core plasma pressure is much smaller than the hot plasma pressure and can be ignored. The perturbed parallel and perpendicular pressures for hot plasma component can be written as

$$\begin{aligned}
& \begin{pmatrix} \delta P_{\parallel h} \\ \delta P_{\perp h} \end{pmatrix} = -\frac{i \mathbf{B} \times \nabla \Phi}{\omega B^2} \cdot \hat{\nabla} \begin{pmatrix} P_{\parallel h} \\ P_{\perp h} \end{pmatrix} \\
& + \frac{\mathbf{B} \cdot \delta \mathbf{B}}{B} \left( \frac{\partial}{\partial B} \right)_{\psi} \begin{pmatrix} P_{\parallel h} \\ P_{\perp h} \end{pmatrix} + \begin{pmatrix} \delta \hat{P}_{\parallel h} \\ \delta \hat{P}_{\perp h} \end{pmatrix},
\end{aligned} \tag{26}$$

where the finite Larmor radius and other kinetic effects such as wave-particle resonances are included in the nonadiabatic perturbed pressures  $\delta \hat{P}_{\perp h}$  and  $\delta \hat{P}_{\parallel h}$ , which were given in the paper by Cheng [1]. Note that on the right-hand side of Eq. (26) the first term represents the convective derivative of plasma pressure, and the second term represents the compressional magnetic field effect associated with pressure nonuniformity along the field line.

Equation (23) becomes

$$\begin{aligned}
& \mathbf{B} \cdot \nabla \left[ \frac{\sigma}{B^2} \mathbf{B} \cdot \nabla (\mathbf{B} \cdot \delta \mathbf{B}) \right] + \frac{\rho \omega^2}{B^2} \mathbf{B} \cdot \delta \mathbf{B} \\
& + \nabla_{\perp}^2 \left( \tau \mathbf{B} \cdot \delta \mathbf{B} - \frac{i \mathbf{B} \times \nabla \Phi \cdot \tilde{\nabla} P_{\perp h}}{\omega B^2} + \delta \hat{P}_{\perp h} \right) \simeq 0,
\end{aligned} \tag{27}$$

which describes the fast magnetosonic (compressional Alfvén) waves and mirror instabilities. Employing the parallel Ampere's law,  $\nabla_{\perp}^2 A_{\parallel} = -\delta J_{\parallel}$  and the parallel electric field definition,  $\mathbf{E}_{\parallel} = -\nabla_{\parallel} \Psi = \nabla_{\parallel} \Phi + i\omega \mathbf{A}_{\parallel}$ , the vorticity equation reduces to

$$\begin{aligned}
& \mathbf{B} \cdot \nabla \left[ \frac{\sigma \nabla_{\perp}^2}{B^2} \mathbf{B} \cdot \nabla (\Phi - \Psi) \right] \\
& + \sum_i \frac{n_i m_i \omega^2}{B^2} \left[ \left( 1 + \frac{3 P_{\perp i} \nabla_{\perp}^2}{4 n_i m_i \omega_{ci}^2} \right) \nabla_{\perp}^2 \Phi + \frac{3 P_{\perp i}}{2 n_i m_i \omega_{ci}} \nabla_{\perp}^2 \delta B_{\parallel} \right] \\
& - \frac{i \omega \mathbf{B} \times \boldsymbol{\kappa}}{B^2} \cdot \nabla \left( \sigma B \delta B_{\parallel} - \frac{i \mathbf{B} \times \nabla \Phi \cdot \tilde{\nabla} P_{\parallel h}}{\omega B^2} - \delta \hat{P}_{\parallel h} \right) \simeq 0,
\end{aligned} \tag{28}$$

which describes mainly the transverse/kinetic Alfvén waves and ballooning instabilities, and the parallel electric field potential  $\Psi$  is given by

$$\Psi \simeq \sum_i \frac{n_i q_i^2}{n_e q_e^2} \left( \frac{T_{\parallel e} \nabla_{\perp}^2 \Phi}{m_i \omega_{ci}^2} + \frac{P_{\perp i} T_{\parallel e} \delta B_{\parallel}}{P_{\parallel i} q_i B} \right). \tag{29}$$

Thus, Eqs. (27), (28) and (29) form the kinetic-MHD eigenmode equations for low frequency waves such as shear/kinetic Alfvén waves, as well as the ballooning and mirror modes, etc.

For low  $\beta$  plasmas the  $\delta B_{\parallel}$  and magnetic field curvature terms in Eq. (27) are usually smaller than the ion inertia and field line bending terms and can be ignored.  $\delta \hat{P}_{\perp h}$  and  $\delta \hat{P}_{\parallel h}$  terms are also small because they appear only in the  $\delta B_{\parallel}$  and magnetic field curvature terms. Then, the kinetic-MHD eigenmode equation for kinetic Alfvén waves can be further simplified and is given by

$$\begin{aligned}
& \mathbf{B} \cdot \nabla \left[ \frac{\sigma \nabla_{\perp}^2}{B^2} \mathbf{B} \cdot \nabla \Upsilon \right] \\
& + \sum_i \frac{n_i m_i \omega^2}{B^2} \left( 1 + \frac{3 P_{\perp i} \nabla_{\perp}^2}{4 n_i m_i \omega_{ci}^2} + \sum_j \frac{n_j q_j^2 T_{\parallel e} \nabla_{\perp}^2}{n_e q_e^2 m_j \omega_{cj}^2} \right) \nabla_{\perp}^2 \Upsilon \simeq 0,
\end{aligned} \tag{30}$$

where  $\Upsilon = \Phi - \Psi$  and the summations over  $i$  and  $j$  are over all core ion species. Equation (30) had been previously derived based on the gyrokinetic theory [14–16] for low  $\beta$  plasmas. The eigenmode equations including full Larmor radius effects have also been derived for kinetic Alfvén wave and kinetic ballooning modes [17, 18].

## VI. SUMMARY AND DISCUSSION

In this paper a nonlinear kinetic-MHD model for studying low frequency multiscale phenomena has been developed by taking advantage of the simplicity of the single fluid MHD model and by properly taking into account core ion finite Larmor radius (FLR) effects and major kinetic effects of energetic particles. The kinetic-MHD model treats the low energy core plasma by a generalized MHD description and energetic particles by kinetic approach such as the gyrokinetic equation, and the coupling between the dynamics of these two components of plasmas is through the plasma pressure in the momentum equation. The major advantage of the kinetic-MHD model is that important kinetic effects can be accurately described with a minimum of modification to the single fluid MHD equations. The generalized MHD model for core plasma includes the parallel electric field, modified perpendicular velocity and gyroviscosity tensor due to core ion FLR effects, which are neglected in the single fluid MHD description. The perturbed core plasma density, velocity and pressure tensor (consisting of the diagonal pressure and gyroviscosity) are determined from the gyro-kinetic equation. From the quasineutrality condition, we obtain the parallel electric field, which arises from the ion polarization drift and parallel electron inertia effects. The generalized Ohm's law contains core ion FLR effects on the parallel electric field and the perpendicular fluid velocity. The kinetic-MHD model is closed by generalized pressure laws, which contain kinetic effects from both the core and energetic plasma components. We note that the generalized MHD equations properly retain important MHD effects such as background density, temperature and magnetic field gradients; magnetic field curvature; large plasma  $\beta$ ; and pressure anisotropy. We also note that important energetic particle kinetic effects such as finite Larmor radius; resonant wave-particle interactions; and bounce resonance are added. These kinetic effects are essential when describing multiscale coupling processes.

From the kinetic-MHD model we derived the kinetic-MHD eigenmode equations for low frequency waves such as shear/kinetic Alfvén waves and ballooning-mirror modes. It is demonstrated that the kinetic effects of parallel electric field and core ion FLR in the dis-

persion relation of KAWs are properly retained. Note that the ion FLR effects on the KAW are not properly included in the popularly employed truncated two-fluid equations without proper gyroviscosity contribution. In the presence of background gradients, ion finite Larmor radius effects couple global MHD disturbances with kinetic Alfvén waves which can strongly interact with ions because the perpendicular wavelength is the order of the ion gyroradius.

The kinetic-MHD model has been successfully applied to study ballooning-mirror instabilities to understand the field-aligned structure and instability threshold of compressional Pc 5 waves in the ring current region. For ballooning-mirror instabilities in the ring current region, the plasma pressure is mainly contributed by hot ions and the core ion FLR effects can be neglected. The hot trapped particle effects stabilize ballooning-mirror modes with symmetric field-aligned  $\delta B_{\parallel}$  structure because hot ions precess very rapidly across the magnetic field and their motion becomes rigid with respect to symmetric ballooning-mirror modes. On the other hand, the bounce motion of hot trapped ions is very rapid and their kinetic effects cancel in a bounce period for antisymmetric ballooning-mirror modes. Thus, the threshold of antisymmetric ballooning-mirror instabilities is determined by the MHD fluid free energy. Thus, ballooning-mirror instabilities represent genuine multiscale kinetic-MHD phenomena; fast time scale trapped particle motion strongly couples to slow time scale MHD modes. We emphasize that the ideal MHD theory predicts an opposite result from our kinetic-MHD theory which is in close agreement with the observations.

Finally, it is worthwhile to point out that we have neglected core plasma diamagnetic drift and wave-particle resonances in our generalized MHD equations. Wave-particle interaction provides wave dissipation and leads to anomalous core plasma transport which can significantly alter the background equilibrium on the transport timescale. Magnetically trapped core particles can also strongly affect wave stability through bounce-resonance effects. Therefore, it is important to pursue in the future a generalized MHD model that also takes into account core plasma diamagnetic drift as well as wave-particle resonance effects.

## ACKNOWLEDGMENTS

We would like to thank Dr. C. T. Hsu for valuable discussion. This work is supported by the NSF grant ATM-9523331 and DoE Contract No. DE-AC02-76-CHO3073.

## REFERENCES

- [1] C. Z. Cheng, *J. Geophys. Res.* **96**, 21,159 (1991).
- [2] E. A. Frieman and L. Chen, *Phys. Fluids* **25**, 502 (1982).
- [3] C. T. Hsu, R. D. Hazeltine, and P. Morrison, *Phys. Fluids* **29**, 1487 (1986).
- [4] H. Berk, C. Z. Cheng, M. N. Rosenbluth, and J. W. V. Dam, *Phys. Fluids* **26**, 2642 (1983).
- [5] C. Z. Cheng and C. S. Lin, *Geophys. Res. Lett.* **14**, 884 (1987).
- [6] C. Z. Cheng and Q. Qian, *J. Geophys. Res.* **99**, 11,193 (1994).
- [7] C. Z. Cheng, Q. Qian, K. Takahashi, and A. T. Y. Lui, *J. Geomag. Geoelectr.* **46**, 997 (1994).
- [8] K. Takahashi, *Adv. Space Res.* **8**, 427 (1988).
- [9] K. Takahashi, J. F. Fennell, E. Amata, and P. R. Higbie, *J. Geophys. Res.* **92**, 5857 (1987).
- [10] K. Takahashi, C. Z. Cheng, R. W. McEntire, and L. M. Kistler, *J. Geophys. Res.* **95**, 977 (1990).
- [11] L. C. Lee, J. R. Johnson, and Z. W. Ma, *J. Geophys. Res.* **99**, 17,405 (1994).
- [12] J. R. Johnson and C. Z. Cheng, *EOS Trans. AGU* **76**, 516 (1995).
- [13] C. K. Goertz and R. A. Smith, *J. Geophys. Res.* **94**, 6581 (1989).
- [14] A. Hasegawa and L. Chen, *Phys. Fluids* **19**, 1924 (1976).
- [15] A. Hasegawa and K. Mima, *Phys. Rev. Lett.* **36**, 1362 (1978).
- [16] C. K. Goertz, *Planet. Space Sci.* **32**, 1387 (1984).
- [17] C. Z. Cheng, N. N. Gorelenkov, and C. T. Hsu, *Nucl. Fusion* **35**, 1639 (1995).

[18] R. L. Lysak and W. Lotko, *J. Geophys. Res.* **101**, 5085 (1995).